

Topological quantum paramagnet in a quantum spin ladder

Darshan G. Joshi* and Andreas P. Schnyder†

Max-Planck-Institute for Solid State Research, D-70569 Stuttgart, Germany

(Dated: January 9, 2018)

It has recently been found that bosonic excitations of ordered media, such as phonons or spinons, can exhibit topologically nontrivial band structures. Of particular interest are magnon and triplon excitations in quantum magnets, as they can easily be manipulated by an applied field. Here we study triplon excitations in an $S=1/2$ quantum spin ladder and show that they exhibit nontrivial topology, even in the quantum-disordered paramagnetic phase. Our analysis reveals that the paramagnetic phase actually consists of two separate regions with topologically distinct triplon excitations. We demonstrate that the topological transition between these two regions can be tuned by an external magnetic field. The winding number that characterizes the topology of the triplons is derived and evaluated. By the bulk-boundary correspondence, we find that the non-zero winding number implies the presence of localized triplon end states. Experimental signatures and possible physical realizations of the topological paramagnetic phase are discussed.

The last decade has witnessed tremendous progress in understanding and classifying topological band structures of fermions [1–4]. Soon after the discovery of fermionic topological insulators [5, 6], it was recognized that bosonic excitations of ordered media can as well exhibit topologically nontrivial bands [7–11]. Such bosonic topological bands have been observed not long ago for photons in dielectric superlattices [12]. Theoretical proposals of topological states in polaritonic systems have been made [13–15], some of which have been observed experimentally [16]. Besides these examples, bosonic band structures are also realized by elementary excitations of quantum spin systems, e.g., by magnons in (anti)ferromagnets or by triplons in dimerized quantum magnets.

The study of these collective spin excitations is enjoying growing interest, due to potential applications for magnonic devices and spintronics [17]. Because magnetic excitations are charge neutral, they are weakly interacting, and therefore exhibit good coherence and support nearly dissipationless spin transport. Moreover, the properties of spin excitations are easily tunable by magnetic fields of moderate strength, as the magnetic interaction scale is in most cases relatively small. Of particular interest are magnetic excitations with nontrivial band structure topology, since they exhibit protected magnon or triplon edge states. This was recently studied for triplons in the ordered phase of the Shastry-Sutherland model [9, 18, 19] and for magnons in an ordered pyrochlore antiferromagnet [20] as well as in an ordered honeycomb ferromagnet [21]. However, the development of a comprehensive topological band theory for magnetic excitations is still in its infancy. Specifically, it has remained unclear whether topological spin excitations can exist also in quantum disordered paramagnets.

In this paper, we address this question by considering, as a prototypical example, the paramagnetic phase of an $S=1/2$ quantum spin ladder with strong spin-orbit coupling. The considered spin ladder model describes a large

class of well studied compounds, called coupled-dimer magnets [22], which have two antiferromagnetically coupled spins per crystallographic unit cell (see Fig. 1). Due to the strong antiferromagnetic exchange coupling within each unit cell, the magnetic ground state of these compounds is a dimer quantum paramagnet, where the two spins in each unit cell form a spin singlet. Examples of $S=1/2$ spin ladder materials include NaV_2O_5 [23], $\text{Bi}(\text{Cu}_{1-x}\text{Zn}_x)_2\text{PO}_6$ [24], and the cuprates SrCu_2O_3 [25], CaCu_2O_3 [26], BiCu_2PO_6 [27], and $\text{LaCuO}_{2.5}$ [28]. Particularly interesting among these is BiCu_2PO_6 , since it exhibits strong spin-orbit couplings, which lead to spin-anisotropic even-parity exchange couplings as well as odd-parity Dzyaloshinskii-Moriya (DM) interactions. As we will show, the latter gives rise to topologically nontrivial triplon excitations.

The elementary low-energy excitations of coupled-dimer magnets correspond to breaking a singlet dimer into a spin-1 triplet state. These excitations are called *triplons* and can be viewed as bosonic quasiparticles with $S=1$. In the absence of spin-orbit coupling the three

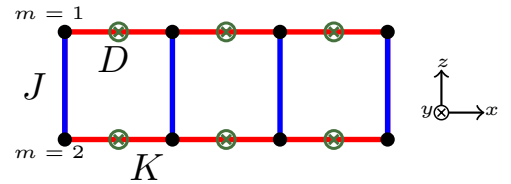


FIG. 1. Schematic representation of the exchange interactions in the quantum spin ladder described by Eq. (1). The spins are shown as black circles, blue lines represent intra-dimer exchange (J), and red lines inter-dimer interactions (K). The DM interaction (D), indicated in green, points in the y -direction into the plane of the ladder. In addition, the model exhibits an even-parity spin-anisotropic interaction (Γ), which arises along with the odd-parity DM interaction due to spin-orbit coupling.

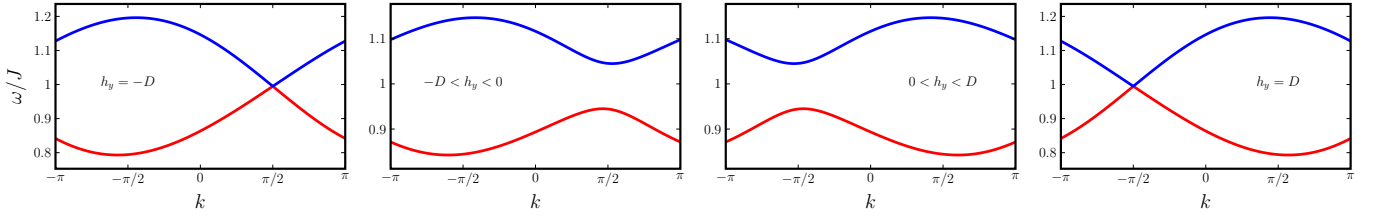


FIG. 2. Triplon bands (t_x and t_z) obtained from \mathcal{H}_k , Eq. (2), are plotted for different h_y . We see that the gap between the two modes vanishes to form a Dirac point at $h_y = \pm D$. Everywhere else in the dimer-quantum-paramagnetic phase, the two modes do not touch each other. For $|h_y| < D$ the phase is topologically non-trivial, else it is trivial. The parameters used are $D/J = \Gamma/J = 0.1$ and $K/J = 0.01$.

triplet states are degenerate, due to $SU(2)$ spin-rotation symmetry. For spin-ladder compounds with heavy elements, however, strong spin-orbit interactions lead to antisymmetric DM couplings, which split the triplon band into multiple dispersive bands. We find that these triplon bands can have nontrivial topological character, which can be tuned by an applied field. In the topologically nontrivial phase, which we call *topological quantum paramagnet*, the spin-ladder exhibits triplon end-states with fractional particle number (see Figs. 3 and 4). We show that these end-states are protected by a nonzero winding number and determine their experimental signatures in heat-transport and neutron-scattering measurements.

Spin model and triplon description.— We consider a spin-1/2 frustrated quantum spin ladder, whose lattice geometry and interactions are illustrated in Fig. 1. The corresponding Hamiltonian is given by

$$\begin{aligned} \mathcal{H} = & J \sum_i \vec{S}_{1i} \cdot \vec{S}_{2i} + K \sum_i [\vec{S}_{1i} \cdot \vec{S}_{1i+1} + \vec{S}_{2i} \cdot \vec{S}_{2i+1}] \\ & + D \sum_i [S_{1i}^z S_{1i+1}^x - S_{1i}^x S_{1i+1}^z + S_{2i}^z S_{2i+1}^x - S_{2i}^x S_{2i+1}^z] \\ & + \Gamma \sum_i [S_{1i}^z S_{1i+1}^x + S_{1i}^x S_{1i+1}^z + S_{2i}^z S_{2i+1}^x + S_{2i}^x S_{2i+1}^z] \\ & + h_y \sum_i [S_{1i}^y + S_{2i}^y], \end{aligned} \quad (1)$$

where, i denotes the dimer site, 1, 2 label the two legs of the ladder, J is the antiferromagnetic intra-dimer coupling, and K is the inter-dimer Heisenberg interaction. Spin-orbit coupling gives rise to the odd-parity DM interaction D and the even-parity spin-anisotropic inter-dimer coupling Γ . We assume that the two legs of the ladder are equivalent by symmetry. Likewise, all the rungs are taken to be equivalent. Therefore, the only symmetry allowed DM term is the inter-dimer DM interaction in the y -direction between the spins along the legs of the ladder [29]. The even-parity spin-anisotropic interaction Γ is of similar form as the DM term, but its direction is not fixed by lattice symmetries. For simplicity, we assume that the Γ term points in the same direction as the DM interaction; in the Supplemental Material we consider the case where the Γ term points along the z direction. In

Eq. (1) we have also included a small magnetic field h_y perpendicular to the ladder plane, which provides a handle to induce a topological transition.

For dominant $J > 0$, the spins within each unit cell of the spin ladder form a singlet and a dimer-quantum-paramagnet is realized. Throughout this paper we shall be interested in this phase only. This phase has three gapped excitations corresponding to the three possible spin-1 triplet excited states on each dimer. To describe these elementary triplon excitations, we employ the bond-operator formalism [30], which allows us to represent the spin operators in Eq. (1) in terms of triplon creation and annihilation operators t_γ^\dagger and t_γ ($\gamma = x, y, z$) [31]. For a given dimer these triplon operators are defined as $t_\gamma^\dagger |t_0\rangle = |t_\gamma\rangle$ ($\gamma = x, y, z$), where $|t_0\rangle = [|\uparrow\downarrow\rangle - |\downarrow\uparrow\rangle]/\sqrt{2}$ is the singlet state, while $|t_x\rangle = -[|\uparrow\uparrow\rangle - |\downarrow\downarrow\rangle]/\sqrt{2}$, $|t_y\rangle = i[|\uparrow\uparrow\rangle + |\downarrow\downarrow\rangle]/\sqrt{2}$, and $|t_z\rangle = [|\uparrow\downarrow\rangle + |\downarrow\uparrow\rangle]/\sqrt{2}$ are the spin-1 triplet states. Rewriting Eq. (1) in terms of t_γ and t_γ^\dagger yields an interacting bosonic Hamiltonian describing the dynamics of the triplons [31]. For simplicity, we consider here only the bilinear part of this triplon Hamiltonian. This is known as the *harmonic approximation* [32]. As it turns out, at the harmonic level the t_y triplon mode is decoupled from the other two triplons. We therefore focus only on the t_x and t_z excitations, whose dynamics in momentum space is given by [31]

$$\mathcal{H}_k = \frac{1}{2} \sum_k \Psi_k^\dagger \mathcal{M}_k \Psi_k, \quad (2a)$$

with the spinor $\Psi_k = (t_{kx}, t_{kz}, t_{-kx}^\dagger, t_{-kz}^\dagger)^T$ and the 4×4 matrix

$$\mathcal{M}_k = \begin{bmatrix} H_1(k) & H_2(k) \\ H_2^\dagger(k) & H_1^T(-k) \end{bmatrix}. \quad (2b)$$

The diagonal and off-diagonal parts of \mathcal{M}_k read

$$H_1(k) = (J + K \cos(k)) \mathbb{1} + \vec{d} \cdot \vec{\sigma}, \quad (3a)$$

$$H_2(k) = -K e^{-ik} \mathbb{1} - \vec{x} \cdot \vec{\sigma}, \quad (3b)$$

with the vectors

$$\vec{d} \equiv \{d_1, d_2, d_3\} = \{\Gamma \cos(k), -D \sin(k) - h_y, 0\}, \quad (3c)$$

$$\vec{x} \equiv \{x_1, x_2, x_3\} = \{\Gamma \cos(k), -D \sin(k), 0\}, \quad (3d)$$

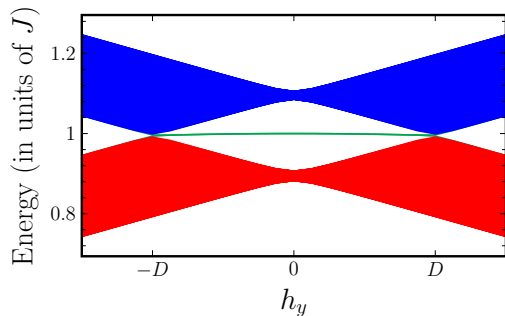


FIG. 3. Band structure of the quantum spin ladder, Eq. (2), with open ends. Protected end states (green line) appear in the topological paramagnetic phase, $|h_y| < D$. Parameters used are the same as in Fig. 2.

where $\mathbb{1}$ is the 2×2 identity matrix, $\iota = \sqrt{-1}$ and $\vec{\sigma} \equiv \{\sigma_1, \sigma_2, \sigma_3\}$ are the three Pauli matrices.

Triplon bands and protected end states.— The triplon bands of Hamiltonian (2) are obtained by use of a bosonic Bogoliubov transformation [33–35], which amounts to diagonalizing the non-Hermitian matrix $\Sigma\mathcal{M}_k$, where $\Sigma = \text{diag}(\mathbb{1}, -\mathbb{1})$. In Fig. 2 we show the typical triplon dispersions for different values of the tuning parameter h_y . Both triplon modes are gapped in the entire dimer-quantum-paramagnetic phase. Moreover, the two triplons do not touch each other, except at $h_y = \pm D$, where they touch linearly. This observation suggests that at $h_y = \pm D$ there occurs a topological phase transition, which separates a trivial phase from a topological one.

To confirm this conjecture, we study the edge states of Hamiltonian \mathcal{H}_k , whose presence indicates the topological character of the triplon bands. For that purpose we determine the eigenenergies and eigenmodes of \mathcal{H}_k in real space with open boundary conditions. Figure 3 displays the so-obtained spectrum as a function of h_y . We also compute the energy-integrated local density of states (LDOS) of \mathcal{H}_k , by adding the contributions from the lower triplon band and from the end states with energies in between the two triplon bands. To reveal the existence of end states we subtract the LDOS of \mathcal{H}_k with periodic boundary conditions ρ_0 from the LDOS with open boundary conditions ρ . The resulting triplon end-state density profile $\rho - \rho_0$ is plotted in Fig. 4 for different values of h_y . From Fig. 3 we clearly see that for $|h_y| < D$ the spectrum contains, besides the bulk triplon bands (red and blue), an additional state (green) with energy in between the two triplons. Figure 4 shows that this in-gap state is exponentially localized at the two ends of the spin ladder. Hence, we conclude that the paramagnetic phase of $S=1/2$ quantum spin ladders is subdivided into a trivial phase ($|h_y| > D$) and a topological phase ($|h_y| < D$) [36]. We call the latter a *topological quantum paramagnet* [37], which is characterized by a non-zero winding number, as we will show below.

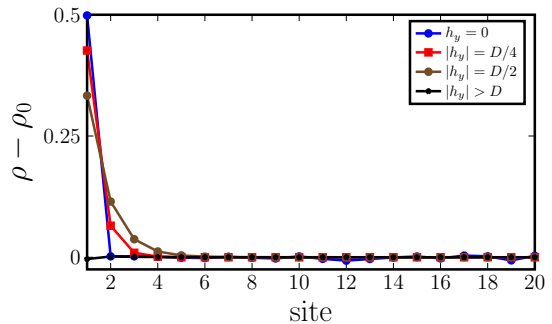


FIG. 4. Triplon end-state density profile $\rho - \rho_0$ plotted in the topological paramagnetic phase, $|h_y| < D$, near one of the ladder ends. In the topologically trivial phase, $|h_y| > D$, the end states are absent (black trace). Parameters used are the same as in Fig. 2.

But before doing so, let us examine the area under the peaks in the triplon end-state density profile of Fig. 4. We find that it is zero in the trivial phase, while in the topological phase it takes on the fractional value $1/2$. This fractional value is reminiscent of the charge $e/2$ end states in the Su-Schrieffer-Heeger model [38] and is intimately connected to the nontrivial topology of the system [2]. Physically, the fractional value hints towards a fractionalized nature of the triplon end states. However, unlike the SSH model, here we are dealing with bosons and it is not straightforward to establish this connection. This will be addressed in future work.

Winding number.— We now show that the topological quantum paramagnetic phase is characterized by a non-zero winding number. Although the problem at hand is seemingly similar to a one-dimensional fermionic topological insulator, we find that the calculation of the winding number proceeds along quite different lines than in the fermionic case. Recall that in order to compute the winding number of fermionic systems, one first needs to identify the chiral symmetry operator and transform the Hamiltonian to a basis wherein the chiral symmetry operator is diagonal. This results in a block off-diagonal Hamiltonian, which is then used to calculate the winding number [3, 4]. For our bosonic model, we find that Eq. (2) can be deformed into a chiral symmetric Hamiltonian, i.e., for $K = 0$ we have $\{\mathbb{1} \otimes \sigma_3, \mathcal{M}_k - J\mathbb{1} \otimes \mathbb{1}\} = 0$, since σ_3 anticommutes with $H_1 - (J + K \cos(k))\mathbb{1}$ and with $H_2 + Ke^{-ik}\mathbb{1}$. However, this observation is not very helpful for two reasons: (i) the symmetry operator is already diagonal and (ii) the eigenmodes of our model are not given by \mathcal{M}_k , but rather by $\Sigma\mathcal{M}_k$.

Hence, we need to find another way to bring $\Sigma\mathcal{M}_k$ into block off-diagonal form. To that end, let us consider the

transformation with the unitary matrix

$$U = \begin{bmatrix} 0 & 0 & 1 & 0 \\ 1 & 0 & 0 & 0 \\ 0 & 0 & 0 & 1 \\ 0 & 1 & 0 & 0 \end{bmatrix}. \quad (4)$$

Under the action of U , the relevant matrix $\Sigma\mathcal{M}_k$ transforms as

$$\tilde{\mathcal{M}}_k = U^\dagger (\Sigma\mathcal{M}_k) U = \begin{bmatrix} \mathcal{A}_k & \mathcal{D}_{1k} \\ \mathcal{D}_{2k} & \mathcal{A}_k \end{bmatrix}, \quad (5a)$$

where

$$\mathcal{A}_k = \begin{bmatrix} J + K \cos(k) & -Ke^{-\iota k} \\ Ke^{\iota k} & -J - K \cos(k) \end{bmatrix}, \quad (5b)$$

and the off-diagonal blocks are given by

$$\mathcal{D}_{1k} = \begin{bmatrix} x_1 + \iota(x_2 - h_y) & -x_1 - \iota x_2 \\ x_1 + \iota x_2 & -x_1 - \iota(x_2 + h_y) \end{bmatrix}, \quad (5c)$$

$$\mathcal{D}_{2k} = \begin{bmatrix} x_1 - \iota(x_2 - h_y) & -x_1 + \iota x_2 \\ x_1 - \iota x_2 & -x_1 + \iota(x_2 + h_y) \end{bmatrix}. \quad (5d)$$

Although $\tilde{\mathcal{M}}_k$ is not block off-diagonal, note that the diagonal block \mathcal{A}_k only leads to an overall energy shift (same for both modes) and small variations in the shape of the modes, but does not alter the topological properties. This is most easily seen by noting that the difference in the triplon energy spectrum with or without the anomalous terms $\mathcal{H}_2(k)$ is negligible. So let us focus on \mathcal{D}_{1k} and \mathcal{D}_{2k} . In a way similar to the fermionic case, we can define the winding number as

$$\mathcal{W} = \frac{1}{2} \frac{1}{4\pi\iota} \int_{BZ} dk \text{Tr} [\mathcal{D}^{-1} \partial_k \mathcal{D} - (\mathcal{D}^\dagger)^{-1} \partial_k \mathcal{D}^\dagger], \quad (6)$$

where $\mathcal{D} = (\mathcal{D}_{1k} + \mathcal{D}_{2k}^\dagger)/2$. We note that the factor 1/2 in Eq. (6) is due to the prefactor 1/2 in Eq. (S18a). The winding number \mathcal{W} is quantized to integer values and evaluates to $\mathcal{W} = -1$ in the topological quantum paramagnetic phase $|h_y| < D$, see Fig. 5. By the bulk-boundary correspondence, the non-zero winding number leads to the protection of the triplon end-states of Fig. 2.

Conclusions and implications for experiments.— We have studied topological properties of S=1/2 quantum spin ladders with strong spin-orbit coupling and have shown that the quantum-disordered paramagnetic state of these spin ladders subdivides into a trivial and a topological phase. The latter is, what we call, a topological quantum paramagnet, since it exhibits topologically non-trivial triplon excitations. It should be noted that there is no qualitative difference between the ground states in the two phases. The topological aspects feature only in the triplon excitation modes. The phase transition between the topological and the trivial quantum paramagnet can be tuned by an applied field and occurs when two

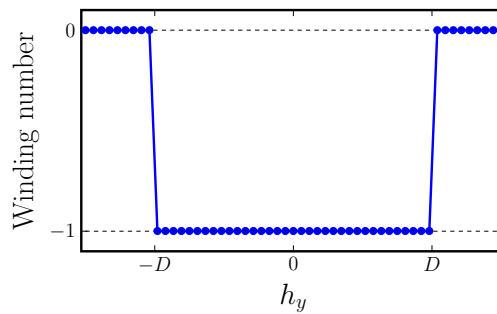


FIG. 5. Winding number \mathcal{W} , Eq. (6), as a function of applied field h_y . In the topological paramagnetic phase, $|h_y| < D$, \mathcal{W} evaluates to -1 , which, by the bulk-boundary correspondence, leads to the appearance of triplon end states, cf. Figs. 3 and 4. Parameters used are the same as in Fig. 2.

triplon modes touch, forming a Dirac point. The topological quantum paramagnet has a non-trivial winding number, which leads to protected triplon end states with fractional particle number 1/2.

We expect that the topological quantum paramagnetic phase exists in many spin ladder compounds, even for relatively weak spin-orbit interactions [39]. The quantum dimer model of Eq. (1) is just one example of a large class of Hamiltonians that all exhibit the same topological phase. It is always possible to add small perturbations to Hamiltonian (1) without changing its topological properties. Based on these considerations we expect that topological triplon bands are quite ubiquitous. A particularly promising candidate material for observing topological triplons is the strongly spin-orbit coupled spin ladder BiCu_2PO_6 , for which field induced phase transitions have recently been investigated [27, 40]. To experimentally study the topological phase transition and the evolution of the triplon band structure as a function of applied field one may use neutron scattering experiments. It may even be possible to directly observe the triplon end states using small-angle neutron scattering (SANS). In fact, our calculations show that the local dynamic spin structure factor exhibits a sharp peak at the triplon end-state energy (see [31]), which should be observable in SANS. Another possibility is to use specific heat measurements to look for the residual $\ln 2$ entropy contributed by the triplon end states.

The triplon interaction terms, arising beyond the harmonic approximation, can in principle result in the intrinsic zero-temperature damping of the triplon modes [41]. This could in particular also apply to the localized end states in the topological phase [42]. However, as long as the gap is greater than $0.5J$, because of energy-momentum constraints, the end states will not decay spontaneously. This is in contrast to the topological edge excitations of ordered magnets [20, 21], which can decay by coupling to the Goldstone modes.

Our findings represent the first step towards the de-

velopment of a comprehensive topological band theory for triplons. Indeed, we expect the topological quantum paramagnet to be a rather commonly occurring phase, which may exist even in two- and three-dimensional quantum magnets. One possible generalization of our work are two-dimensional magnets composed of coupled spin-ladders, which may exhibit dispersing triplon edge modes carrying dissipationless spin current. Besides this, other interesting questions for further study are: (i) the fate of the topological quantum paramagnet at finite temperature and (ii) the study of phase transitions between topological quantum paramagnets and quantum spin liquids.

We thank A. Chernyshev, G. Khaliullin, S. Rachel, H. Takagi, and M. Vojta for useful discussions. A.P.S. is grateful to the KITP at UC Santa Barbara for hospitality during the preparation of this work. This research was supported in part by the National Science Foundation under Grant No. NSF PHY-1125915.

-
- [1] M. Z. Hasan and C. L. Kane, *Rev. Mod. Phys.* **82**, 3045 (2010).
- [2] X.-L. Qi and S.-C. Zhang, *Rev. Mod. Phys.* **83**, 1057 (2011).
- [3] A. P. Schnyder, S. Ryu, A. Furusaki, and A. W. W. Ludwig, *Phys. Rev. B* **78**, 195125 (2008).
- [4] C.-K. Chiu, J. C. Y. Teo, A. P. Schnyder, and S. Ryu, *Rev. Mod. Phys.* **88**, 03005 (2016), URL <https://link.aps.org/doi/10.1103/RevModPhys.88.035005>.
- [5] M. König, S. Wiedmann, C. Brüne, A. Roth, H. Buhmann, L. W. Molenkamp, X.-L. Qi, and S.-C. Zhang, *Science* **318**, 766 (2007), ISSN 0036-8075, <http://science.sciencemag.org/content/318/5851/766.full.pdf> URL <http://science.sciencemag.org/content/318/5851/766>.
- [6] D. Hsieh, Y. Xia, D. Qian, L. Wray, J. H. Dil, F. Meier, J. Osterwalder, L. Patthey, J. G. Checkelsky, N. P. Ong, et al., *Nature* **460**, 1101 (2009), URL <http://dx.doi.org/10.1038/nature08234>.
- [7] R. Shindou, R. Matsumoto, S. Murakami, and J.-i. Ohe, *Phys. Rev. B* **87**, 174427 (2013), URL <https://link.aps.org/doi/10.1103/PhysRevB.87.174427>.
- [8] L. Zhang, J. Ren, J.-S. Wang, and B. Li, *Phys. Rev. B* **87**, 144101 (2013), URL <https://link.aps.org/doi/10.1103/PhysRevB.87.144101>.
- [9] J. Romhányi, K. Penc, and R. Ganesh, *Nature Communications* **6** (2015), URL <http://dx.doi.org/10.1038/ncomms7805>.
- [10] V. Peano, C. Brendel, M. Schmidt, and F. Marquardt, *Phys. Rev. X* **5**, 031011 (2015), URL <https://link.aps.org/doi/10.1103/PhysRevX.5.031011>.
- [11] L. Lu, J. D. Joannopoulos, and M. Soljacic, *Nat Photon* **8**, 821 (2014), URL <http://dx.doi.org/10.1038/nphoton.2014.248>.
- [12] Z. Wang, Y. Chong, J. D. Joannopoulos, and M. Soljacic, *Nature* **461**, 772 (2009), URL <http://dx.doi.org/10.1038/nature08293>.
- [13] D. D. Solnyshkov, A. V. Nalitov, and G. Malpuech, *Phys. Rev. Lett.* **116**, 046402 (2016), URL <https://link.aps.org/doi/10.1103/PhysRevLett.116.046402>.
- [14] T. Jacqumin, I. Carusotto, I. Sagnes, M. Abbarchi, D. D. Solnyshkov, G. Malpuech, E. Galopin, A. Lemaître, J. Bloch, and A. Amo, *Phys. Rev. Lett.* **112**, 116402 (2014), URL <https://link.aps.org/doi/10.1103/PhysRevLett.112.116402>.
- [15] O. Bleu, S. D. D., and G. G. Malpuech, *Phys. Rev. B* **93**, 085438 (2016), URL <https://link.aps.org/doi.org/10.1103/PhysRevB.93.085438>.
- [16] P. St-Jean et al., *Nature Photonics* (2017).
- [17] B. Lenk, H. Ulrichs, F. Garbs, and M. Mnzenberg, *Physics Reports* **507**, 107 (2011), ISSN 0370-1573, URL <http://www.sciencedirect.com/science/article/pii/S0370157311001694>.
- [18] P. A. McClarty et al., *Nature Physics* (2017), URL <http://dx.doi.org/10.1038/nphys4117>.
- [19] M. Malki and K. P. Schmidt, *Phys. Rev. B* **95**, 195137 (2017), URL <https://link.aps.org/doi.org/10.1103/PhysRevB.95.195137>.
- [20] F.-Y. Li, Y.-D. Li, Y. B. Kim, L. Balents, Y. Yu, and G. Chen, *Nature Communications* **7** (2016), URL <http://dx.doi.org/10.1038/ncomms12691>.
- [21] S. K. Kim, H. Ochoa, R. Zarzuela, and Y. Tserkovnyak, *Phys. Rev. Lett.* **117**, 227201 (2016), URL <https://link.aps.org/doi/10.1103/PhysRevLett.117.227201>.
- [22] E. Dagotto and T. M. Rice, *Science* **271**, 618 (1996), ISSN 0036-8075, <http://science.sciencemag.org/content/271/5249/618.full.pdf>, URL <http://science.sciencemag.org/content/271/5249/618>.
- [23] M. Isobe and Y. Ueda, *Journal of the Physical Society of Japan* **65**, 1178 (1996).
- [24] O. Mentr, E. M. Ketatni, M. Colmont, M. Huv, F. Abraham, and V. Petricek, *Journal of the American Chemical Society* **128**, 10857 (2006), pMID: 16910681, <http://dx.doi.org/10.1021/ja0631091>, URL <http://dx.doi.org/10.1021/ja0631091>.
- [25] M. Azuma, Z. Hiroi, M. Takano, K. Ishida, and Y. Kitaoka, *Phys. Rev. Lett.* **73**, 3463 (1994), URL <https://link.aps.org/doi/10.1103/PhysRevLett.73.3463>.
- [26] V. Kiryukhin, Y. J. Kim, K. J. Thomas, F. C. Chou, R. W. Erwin, Q. Huang, M. A. Kastner, and R. J. Birgeneau, *Phys. Rev. B* **63**, 144418 (2001), URL <https://link.aps.org/doi/10.1103/PhysRevB.63.144418>.
- [27] Y. Kohama, S. Wang, A. Uchida, K. Prsa, S. Zvyagin, Y. Skourski, R. D. McDonald, L. Balicas, H. M. Ronnow, C. Rüegg, et al., *Phys. Rev. Lett.* **109**, 167204 (2012), URL <https://link.aps.org/doi/10.1103/PhysRevLett.109.167204>.
- [28] Z. Hiroi and M. Takano, *Nature* **377**, 41 (1995), URL <http://dx.doi.org/10.1038/377041a0>.
- [29] Strictly speaking, there could also be DM interactions perpendicular to the rung, such that it lies in the ladder plane and is in alternating directions on adjacent rungs. This has been studied, for example, by S. Miyahara et al., *Phys. Rev. B* **75**, 184402 (2007). However, this leads to condensation of triplons, in other words, to a symmetry broken phase, and so we do not consider it here.
- [30] S. Sachdev and R. N. Bhatt, *Phys. Rev. B* **41**, 9323 (1990), URL <https://link.aps.org/doi/10.1103/PhysRevB.41.9323>.
- [31] See Supplemental Material for the derivation of the triplon Hamiltonian, the computation of the local density

- of states, the dynamic structure factor, and the winding number. It includes Refs. [43, 44].
- [32] Inside the paramagnetic phase and away from a magnetic quantum critical point, the triplon density is small and hence triplon interactions can be neglected. In general, the harmonic approximation is controlled in large dimensions, both in the paramagnetic as well as inside the magnetically ordered phases, as shown in Refs. [45, 46]. That said, small interactions cannot change the topology of the quantum spin ladder, since they respect the same symmetries of the spin Hamiltonian, which are given by the lattice.
- [33] J.-P. Blaizot and G. Ripka, *Quantum Theory of Finite Systems* (MIT press, Cambridge, 1986).
- [34] E. R. Mucciolo, A. H. Castro Neto, and C. Chamon, Phys. Rev. B **69**, 214424 (2004), URL <https://link.aps.org/doi/10.1103/PhysRevB.69.214424>.
- [35] S. Wessel and I. Milat, Phys. Rev. B **71**, 104427 (2005), URL <https://link.aps.org/doi/10.1103/PhysRevB.71.104427>.
- [36] Note that there is no qualitative difference between the ground states of the topologically trivial and topologically non-trivial phases. In both the phases, there are triplon excitations over the singlet product state. The topological aspect, which distinguishes the two phases, features in these triplon bands and is amenable to experimental detection as discussed in the text. However, unlike in fermionic topological systems (e.g., topological superconductors), these experimental signatures are observed at an elevated energy rather than at zero energy.
- [37] Note that the topological quantum paramagnet studied in this Letter is different from a quantum spin liquid, which is characterized by fractional bulk excitations and topological order. Three-dimensional quantum spin liquids with fractional bulk excitations have recently been studied in Refs. [47, 48] using field theory methods.
- [38] A. J. Heeger, S. Kivelson, J. R. Schrieffer, and W. P. Su, Rev. Mod. Phys. **60**, 781 (1988), URL <https://link.aps.org/doi/10.1103/RevModPhys.60.781>.
- [39] The topological phase occurs whenever the DM interaction D is larger than the applied magnetic field h_y . It should be noted, however, that the localized end states are most clearly visible only in the regime $K < D$, where there exists a full gap between the two triplon bands. In contrast, in the regime $K > D$ the triplon end states overlap with the bulk states and are therefore broadened and decay algebraically into the bulk.
- [40] L. Splinter, N. A. Drescher, H. Krull, and G. S. Uhrig, Phys. Rev. B **94**, 155115 (2016), URL <https://link.aps.org/doi/10.1103/PhysRevB.94.155115>.
- [41] M. E. Zhitomirsky and A. L. Chernyshev, Rev. Mod. Phys. **85**, 219 (2013), URL <https://arxiv.org/abs/1703.03566>.
- [42] A. L. Chernyshev and P. A. Maksimov, Phys. Rev. Lett. **117**, 187203 (2016), URL <https://link.aps.org/doi/10.1103/PhysRevLett.117.187203>.
- [43] A. Collins, C. J. Hamer, and Z. Weihong, Phys. Rev. B **74**, 144414 (2006), URL <https://link.aps.org/doi/10.1103/PhysRevB.74.144414>.
- [44] J. Romhányi, K. Totsuka, and K. Penc, Phys. Rev. B **83**, 024413 (2011), URL <https://link.aps.org/doi/10.1103/PhysRevB.83.024413>.
- [45] D. G. Joshi, K. Coester, K. P. Schmidt, and M. Vojta, Phys. Rev. B **91**, 094404 (2015), URL <https://link.aps.org/doi/10.1103/PhysRevB.91.094404>.
- [46] D. G. Joshi and M. Vojta, Phys. Rev. B **91**, 094405 (2015), URL <https://link.aps.org/doi/10.1103/PhysRevB.91.094405>.
- [47] A. Vishwanath and T. Senthil, Phys. Rev. X **3**, 011016 (2013), URL <https://link.aps.org/doi/10.1103/PhysRevX.3.011016>.
- [48] C. Wang, A. Nahum, and T. Senthil, Phys. Rev. B **91**, 195131 (2015), URL <https://link.aps.org/doi/10.1103/PhysRevB.91.195131>.

Supplemental material: Topological quantum paramagnet in a quantum spin ladder

Darshan G. Joshi and Andreas P. Schnyder

Max-Planck-Institute for Solid State Research, D-70569 Stuttgart, Germany

TRIPLON HAMILTONIAN

As discussed in the main text, the spin-1 excitations on top of a singlet state are described as bosonic quasi-particles, triplons, within the bond-operator theory [S1]. The spin operators can be thus expressed as follows in terms of triplon operators:

$$S_{1,2i}^\alpha = \frac{1}{2} [\pm t_{i\alpha}^\dagger P_i \mp \iota P_i t_{i\alpha} - \iota \epsilon_{\alpha\beta\gamma} t_{i\beta}^\dagger t_{i\gamma}], \quad (\text{S1})$$

$$\vec{S}_{1i} \cdot \vec{S}_{2i} = -\frac{3}{4} + \sum_\alpha t_{i\alpha}^\dagger t_{i\alpha}. \quad (\text{S2})$$

Here, t_α ($\alpha = x, y, z$) are the triplon operators and $P_i = 1 - \sum_\alpha t_{i\alpha}^\dagger t_{i\alpha}$ is the projection operator [S2] which takes care of the Hilbert-space constraint, i.e., no more than one boson per dimer. Note that the appearance of $\iota = \sqrt{-1}$ in the above equation is due the convention in which the triplon operators are time-reversal invariant [S3]. Inserting this in the spin Hamiltonian [Eq. (1)] in the main text we obtain the triplon Hamiltonian as follows:

$$\begin{aligned} \mathcal{H} = & -\frac{3}{4} JN + J \sum_{i\alpha} t_{i\alpha}^\dagger t_{i\alpha} \\ & + \frac{K}{2} \sum_{i\alpha} [t_{i\alpha}^\dagger P_i P_{i+1} t_{i+1\alpha} - t_{i\alpha}^\dagger P_i t_{i+1\alpha}^\dagger P_{i+1} + H.c.] \\ & + \frac{D}{2} \sum_i [t_{iz}^\dagger P_i P_{i+1} t_{i+1x} - t_{iz}^\dagger P_i t_{i+1x}^\dagger P_{i+1} \\ & \quad - t_{ix}^\dagger P_i P_{i+1} t_{i+1z} + t_{ix}^\dagger P_i t_{i+1z}^\dagger P_{i+1} + H.c.] \\ & + \frac{\Gamma}{2} \sum_i [t_{iz}^\dagger P_i P_{i+1} t_{i+1x} - t_{iz}^\dagger P_i t_{i+1x}^\dagger P_{i+1} \\ & \quad + t_{ix}^\dagger P_i P_{i+1} t_{i+1z} - t_{ix}^\dagger P_i t_{i+1z}^\dagger P_{i+1} + H.c.] \\ & + \iota h_y \sum_i [t_{ix}^\dagger t_{iz} - t_{iz}^\dagger t_{ix}] \end{aligned} \quad (\text{S3})$$

where, N is number of dimer sites. Here on, we shall consider only the bilinear piece in the above interacting Hamiltonian. This is known as the *harmonic approximation* and it has been shown that it is a controlled approximation, such that corrections beyond it can be arranged in a systematic expansion in inverse spatial dimension [S4, S5]. So triplon interactions will not qualitatively change the physics discussed here. The bilinear

Hamiltonian is as follows:

$$\begin{aligned} \mathcal{H}_2 = & J \sum_{i\alpha} t_{i\alpha}^\dagger t_{i\alpha} + \frac{K}{2} \sum_{i\alpha} [t_{i\alpha}^\dagger t_{i+1\alpha} - t_{i\alpha}^\dagger t_{i+1\alpha}^\dagger + H.c.] \\ & + \frac{D}{2} \sum_i [t_{iz}^\dagger t_{i+1x} - t_{iz}^\dagger t_{i+1x}^\dagger - t_{ix}^\dagger t_{i+1z} + t_{ix}^\dagger t_{i+1z}^\dagger + H.c.] \\ & + \frac{\Gamma}{2} \sum_i [t_{iz}^\dagger t_{i+1x} - t_{iz}^\dagger t_{i+1x}^\dagger + t_{ix}^\dagger t_{i+1z} - t_{ix}^\dagger t_{i+1z}^\dagger + H.c.] \\ & + \iota h_y \sum_i [t_{ix}^\dagger t_{iz} - t_{iz}^\dagger t_{ix}] \end{aligned} \quad (\text{S4})$$

At the harmonic level, the t_y mode is decoupled from the other two triplon modes. It is straightforward to obtain its dispersion; $\omega_{ky} = \sqrt{(J + K \cos(k))^2 - K^2}$. We shall now on focus only on the t_x and t_z triplon modes, which is discussed in the main text.

LOCAL DENSITY OF STATES

In the main text, we presented the local density of states to establish that the end states were indeed localized at the ends of the ladder. Here we sketch the necessary technical details. As mentioned in the main text, the eigenmodes of the triplon Hamiltonian are obtained by diagonalizing the matrix $\Sigma \mathcal{H}$. This is a non-Hermitian matrix and it is diagonalized in the following way [S6–S8]:

$$\Omega = T^\dagger \mathcal{H} T \quad (\text{S5})$$

where, Ω is the diagonal matrix containing the eigenmodes of the Hamiltonian and

$$T = \begin{bmatrix} U & V \\ V^* & U^* \end{bmatrix} \quad (\text{S6})$$

satisfying the condition,

$$T^\dagger \Sigma T = T \Sigma T^\dagger = \Sigma. \quad (\text{S7})$$

This ensures that the bosonic commutation relations are satisfied. The matrices U and V contain the Bogoliubov coefficients. For an eigenfrequency ω_n ,

$$\Sigma \mathcal{H} |\phi_n\rangle = \omega_n |\phi_n\rangle; \quad |\phi_n\rangle = \begin{bmatrix} u_n \\ v_n^* \end{bmatrix}. \quad (\text{S8})$$

The local density of states as a function of site i is then given by

$$\rho(i) = \sum_{n \in \{\omega_n \leq \omega_0\}} \left[|u_{i,n}|^2 + |u_{i+N,n}|^2 - |v_{i,n}|^2 - |v_{i+N,n}|^2 \right] \quad (\text{S9})$$

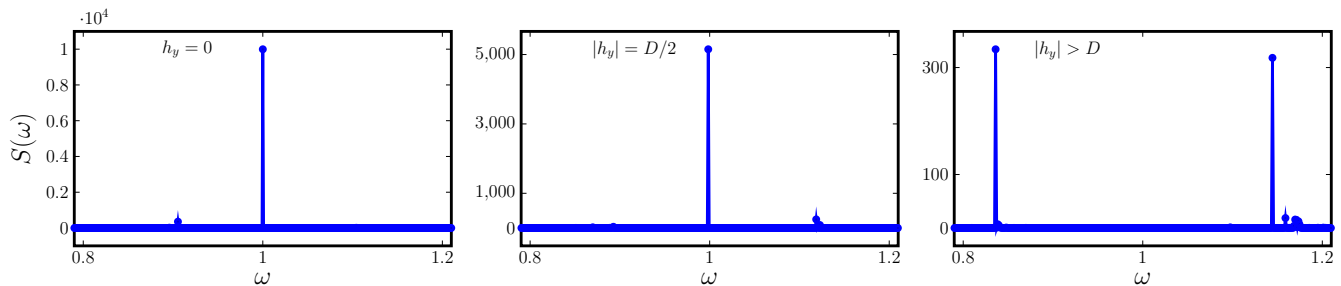


FIG. S1. Dynamic structure factor at $k = 0$ for different values of external field h_y . We see sharp peaks at the end-state energy within the topological-quantum-paramagnetic phase, while these peaks disappear in the trival paramagnetic phase. The parameters used here are $D/J = \Gamma/J = 0.1$ and $K/J = 0.01$.

where, ω_0 is the end-state energy. This is plotted in Fig. 4 in the main text, where we see exponentially localized peaks near the ladder ends inside the topological phase.

WINDING NUMBER

In case of a hopping Hamiltonian in the Dirac form, it is straightforward to calculate the winding number invari-

ant. However, for the model discussed in the main text, we also have anomalous terms. As mentioned in the main text, unlike the fermionic case, it is not straightforward to bring the Hamiltonian in an off-block diagonal form. With the help of a suitable transformation, however, we were able to write down an expression for the winding number [Eq. (6)]. Here we quote the explicit expression obtained after inserting the matrices \mathcal{D}_{1k} and \mathcal{D}_{2k} in Eq. (6) in the main text:

$$\mathcal{W} = \frac{1}{8\pi} \int_{-\pi}^{\pi} \frac{2D\Gamma(-D^2 - \Gamma^2 + (D^2 - \Gamma^2 - 2h_y^2) \cos(2k))}{\Gamma^4 \cos^4(k) + (h_y^2 - D^2 \sin^2(k))^2 + 2\Gamma^2 \cos^2(k)(h_y^2 + D^2 \sin^2(k))} dk \quad (\text{S10})$$

This is plotted in Fig. (5) in the main text. As is evident, the winding number is non zero in the topological quantum paramagnetic phase, while zero in the trivial paramagnetic phase.

Note that although both D and Γ enter the formula for the winding number, the topological phase transition depends only on the relative values of h_y and D . Any non-zero value of Γ is sufficient to keep the topological aspect. For $\Gamma = 0$ or $D = 0$, the winding is always zero and hence there will be no topological quantum paramagnet.

DYNAMIC STRUCTURE FACTOR

We wish to calculate the dynamic structure factor for the ladder with open boundaries to see the signature of the end states. But this means that the crystal momentum is not a good quantum number anymore. So we calculate the *local* dynamic structure factor, which will

correspond to the $k = 0$ contribution in a scattering experiment. The dynamic structure factor,

$$S(k, \omega) = \frac{1}{N} \sum_{i,j} S_{ij} e^{ikr_{ij}}. \quad (\text{S11})$$

So,

$$S(\omega) \equiv S(k = 0, \omega) = \frac{1}{N} \sum_{i,j} S_{ij}, \quad (\text{S12})$$

where $S_{ij} = -\Im \chi_{ij}$, with χ being the spin correlation function and \Im stands for the imaginary part. Owing to the two legs of the ladder, there are two channels for spin-spin correlations: even and odd. Spin-spin correlations in the even (odd) channel are calculated with respect to $\vec{S}_1 \pm \vec{S}_2$. It is straightforward to see that within the single-mode approximation (no continuum contribution) only the odd channel is relevant. After a few steps of algebra we obtain

$$S_{ij}^{xx} = \sum_{m=1}^N \left\{ \delta(\omega - \omega_{mx}) [-v_{i,m}^* u_{j,m}^* + v_{i,m}^* v_{j,m} + u_{i,m} u_{j,m}^* - u_{i,m} v_{j,m}] \right. \\ \left. + \delta(\omega - \omega_{mz}) [-v_{i,m+N}^* u_{j,m+N}^* + v_{i,m+N}^* v_{j,m+N} + u_{i,m+N} u_{j,m+N}^* - u_{i,m+N} v_{j,m+N}] \right\}, \quad (\text{S13})$$

$$S_{ij}^{zz} = \sum_{m=1}^N \left\{ \delta(\omega - \omega_{mx}) [-v_{i+N,m}^* u_{j+N,m}^* + v_{i+N,m}^* v_{j+N,m} + u_{i+N,m} u_{j+N,m}^* - u_{i+N,m} v_{j+N,m}] \right. \\ \left. + \delta(\omega - \omega_{mz}) [-v_{i+N,m+N}^* u_{j+N,m+N}^* + v_{i+N,m+N}^* v_{j+N,m+N} + u_{i+N,m+N} u_{j+N,m+N}^* - u_{i+N,m+N} v_{j+N,m+N}] \right\}. \quad (\text{S14})$$

The structure factor $S(\omega)$ is then obtained by summing all the spin contributions (here, x and z). This is plotted in Fig. (S1). Note that here we have neglected broadening of the lines and so there are only sharp delta peaks. Inside the topological paramagnet, we can see a dominant sharp peak at the end-state energy with smaller peaks (much weaker intensity) from the bulk triplon bands. In the trivial phase there is no such peak at the end-state energy.

ALTERNATIVE MODEL

In the main text we have considered a model where the even-parity term Γ points in the same direction as the DM interaction. However, the direction of the Γ term is not fixed by lattice symmetries. It can also point in some other direction, depending on the arrangement of the atoms in a given compound. But the topological phase is expected to be present for any direction of the Γ term. Here we show this, by considering a model where the Γ term points along the z direction. The corresponding Hamiltonian is given by

$$\mathcal{H} = J \sum_i \vec{S}_{1i} \cdot \vec{S}_{2i} + K \sum_i [\vec{S}_{1i} \cdot \vec{S}_{1i+1} + \vec{S}_{2i} \cdot \vec{S}_{2i+1}] \\ + D \sum_i [S_{1i}^z S_{1i+1}^x - S_{1i}^x S_{1i+1}^z + S_{2i}^z S_{2i+1}^x - S_{2i}^x S_{2i+1}^z] \\ + \Gamma \sum_i [S_{1i}^x S_{1i+1}^y + S_{1i}^y S_{1i+1}^x + S_{2i}^x S_{2i+1}^y + S_{2i}^y S_{2i+1}^x] \\ + h_y \sum_i [S_{1i}^y + S_{2i}^y]. \quad (\text{S15})$$

The main difference between the above model and that considered in the main text [Eq. (1)] is that, here the even-parity spin anisotropic interaction Γ points in different direction compared to that of the odd-parity DM interaction. Using Eq. (S1) and (S2), we obtain the cor-

responding triplon Hamiltonian:

$$\mathcal{H} = -\frac{3}{4} JN + J \sum_{i\alpha} t_{i\alpha}^\dagger t_{i\alpha} \\ + \frac{K}{2} \sum_{i\alpha} [t_{i\alpha}^\dagger P_i P_{i+1} t_{i+1\alpha} - t_{i\alpha}^\dagger P_i t_{i+1\alpha}^\dagger P_{i+1} + H.c.] \\ + \frac{D}{2} \sum_i [t_{iz}^\dagger P_i P_{i+1} t_{i+1z} - t_{iz}^\dagger P_i t_{i+1z}^\dagger P_{i+1} \\ - t_{ix}^\dagger P_i P_{i+1} t_{i+1x} + t_{ix}^\dagger P_i t_{i+1x}^\dagger P_{i+1} + H.c.] \\ + \frac{\Gamma}{2} \sum_i [t_{ix}^\dagger P_i P_{i+1} t_{i+1y} - t_{ix}^\dagger P_i t_{i+1y}^\dagger P_{i+1} \\ + t_{iy}^\dagger P_i P_{i+1} t_{i+1x} - t_{iy}^\dagger P_i t_{i+1x}^\dagger P_{i+1} + H.c.] \\ + \iota h_y \sum_i [t_{ix}^\dagger t_{iz} - t_{iz}^\dagger t_{ix}]. \quad (\text{S16})$$

Keeping only the bilinear piece, which amounts to the harmonic approximation, we obtain

$$\mathcal{H}_2 = J \sum_{i\alpha} t_{i\alpha}^\dagger t_{i\alpha} + \frac{K}{2} \sum_{i\alpha} [t_{i\alpha}^\dagger t_{i+1\alpha} - t_{i\alpha}^\dagger t_{i+1\alpha}^\dagger + H.c.] \\ + \frac{D}{2} \sum_i [t_{iz}^\dagger t_{i+1z} - t_{iz}^\dagger t_{i+1z}^\dagger - t_{ix}^\dagger t_{i+1x} + t_{ix}^\dagger t_{i+1x}^\dagger + H.c.] \\ + \frac{\Gamma}{2} \sum_i [t_{ix}^\dagger t_{i+1y} - t_{ix}^\dagger t_{i+1y}^\dagger + t_{iy}^\dagger t_{i+1x} - t_{iy}^\dagger t_{i+1x}^\dagger + H.c.] \\ + \iota h_y \sum_i [t_{ix}^\dagger t_{iz} - t_{iz}^\dagger t_{ix}]. \quad (\text{S17})$$

In contrast to the model described in the main text, here all the three triplon modes are coupled even at the harmonic level. Even in this case, the quantum paramagnetic phase is split into a topological and a trivial part. The topological phase transition occurring again at $h_y = |D|$. The eigenmodes of the bilinear Hamiltonian [Eq. (S17)] with open boundary condition are plotted in Fig. S2. Apart from the three bulk triplon modes, we also find doubly degenerate end states at each end of the ladder in the topological phase. Interestingly, the

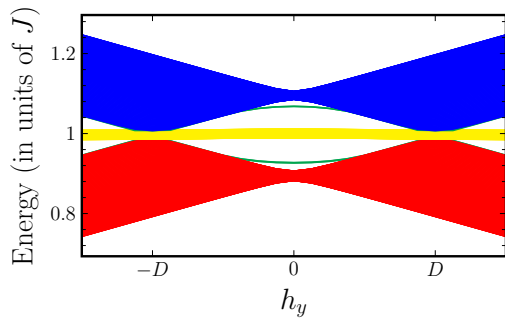


FIG. S2. Band structure for the alternative model, Eq. (S17), with open ends. Protected end states (green line) appear in the topological paramagnetic phase, $|h_y| < D$. In contrast to the model discussed in the main text, the end-state energy varies with h_y and the end states merge with the bulk well before $h_y = |D|$. The parameters used here are $D/J = \Gamma/J = 0.1$ and $K/J = 0.01$.

end-state energy changes as a function of h_y and the end states merge with the bulk triplon bands even before the bulk bands touch each other at $h_y = |D|$.

In this case, we could not find a suitable transformation which will bring the bilinear Hamiltonian [Eq. (S17)], written in momentum space, in an off-block diagonal form. So an expression for the winding number can not be derived. However, we can make some progress by considering only the hopping piece. For small Γ and D the effect of anomalous terms is negligible, such that the full bilinear Hamiltonian is adiabatically connected to the hopping Hamiltonian. The hopping piece in the momentum space is given by

$$\mathcal{H}_{k,hop} = \frac{1}{2} \sum_k \Psi_k^\dagger \mathcal{H}_{1k} \Psi_k, \quad (\text{S18a})$$

with the spinor $\Psi_k = (t_{kx}, t_{ky}, t_{kz})^T$ and the 2×2 matrix

$$H_1(k) = (J + K \cos(k)) \mathbb{1} + \vec{d}' \cdot \vec{L}, \quad (\text{S18b})$$

such that

$$\vec{L} = \left\{ \begin{bmatrix} 0 & 1 & 0 \\ 1 & 0 & 0 \\ 0 & 0 & 0 \end{bmatrix}, \begin{bmatrix} 0 & 0 & i \\ 0 & 0 & 0 \\ -i & 0 & 0 \end{bmatrix}, \begin{bmatrix} 0 & 0 & 0 \\ 0 & 0 & 1 \\ 0 & 1 & 0 \end{bmatrix} \right\} \quad (\text{S18c})$$

satisfy the SU(2) algebra: $[L_i, L_j] = i\epsilon_{ijk} L_k$, and $\vec{d}' = \{\Gamma \cos(k), D \sin(k) + h_y, 0\}$. The winding number corresponding to $\mathcal{H}_{k,hop}$ is easy to evaluate,

$$\mathcal{W} = \frac{1}{2\pi} \left[\int \frac{1}{|d'|^2} (d'_1 d(d'_2) - d'_2 d(d'_1)) \right]. \quad (\text{S19})$$

It is non-zero in the topological quantum paramagnetic phase, $h_y < |D|$, while it is zero in the trivial phase. It is therefore reasonable to assume that even upon including the anomalous terms the topological phase exists. This is also evident from Fig. S2, where we can clearly see end states even in the presence of the anomalous terms.

-
- [S1] S. Sachdev and R. N. Bhatt, Phys. Rev. B **41**, 9323 (1990).
 - [S2] A. Collins, C. J. Hamer, and Zheng Weihong, Phys. Rev. B **74**, 144414 (2006).
 - [S3] J. Romhányi, K. Totsuka, and K. Penc, Phys. Rev. B **83**, 024413 (2011).
 - [S4] D. G. Joshi, K. Coester, K. P. Schmidt, and M. Vojta, Phys. Rev. B **91**, 094404 (2015).
 - [S5] D. G. Joshi and M. Vojta, Phys. Rev. B **91**, 094405 (2015).
 - [S6] J.-P. Blaizot and G. Ripka, *Quantum Theory of Finite Systems* (MIT press, Cambridge, 1986).
 - [S7] E. R. Mucciolo, A. H. C. Neto, and C. Chamon, Phys. Rev. B **69**, 214424 (2004).
 - [S8] S. Wessel and I. Milat, Phys. Rev. B **71**, 104427 (2005).